Numerical study of a normally hyperbolic cylinder in the RTBP

Jacques Féjoz, Marcel Guardia, Pablo Roldán, Vadim Kaloshin

Mechanism of Instability

- Consider the three-body problem consisting of the Sun, Jupiter, and an Asteroid which moves on (approximate) ellipses.
- A possible source of instabilities are *orbital resonances* between the frequencies of Jupiter and the Asteroid.
- Jupiter and the Asteroid are regularly in the same relative position. Over a long time interval, Jupiter's influence piles up and modifies the eccentricity of the Asteroid.
- According to Kepler's third law, resonances take place when the semi-major axis a satisfies

$$a^{3/2} \approx \frac{\omega_J}{\omega_A} \in \mathbb{Q}.$$

Kirkwood Gaps

- The Asteroid Belt is located between the orbits of Mars and Jupiter. The distribution of asteroids presents several gaps precisely at the resonances.

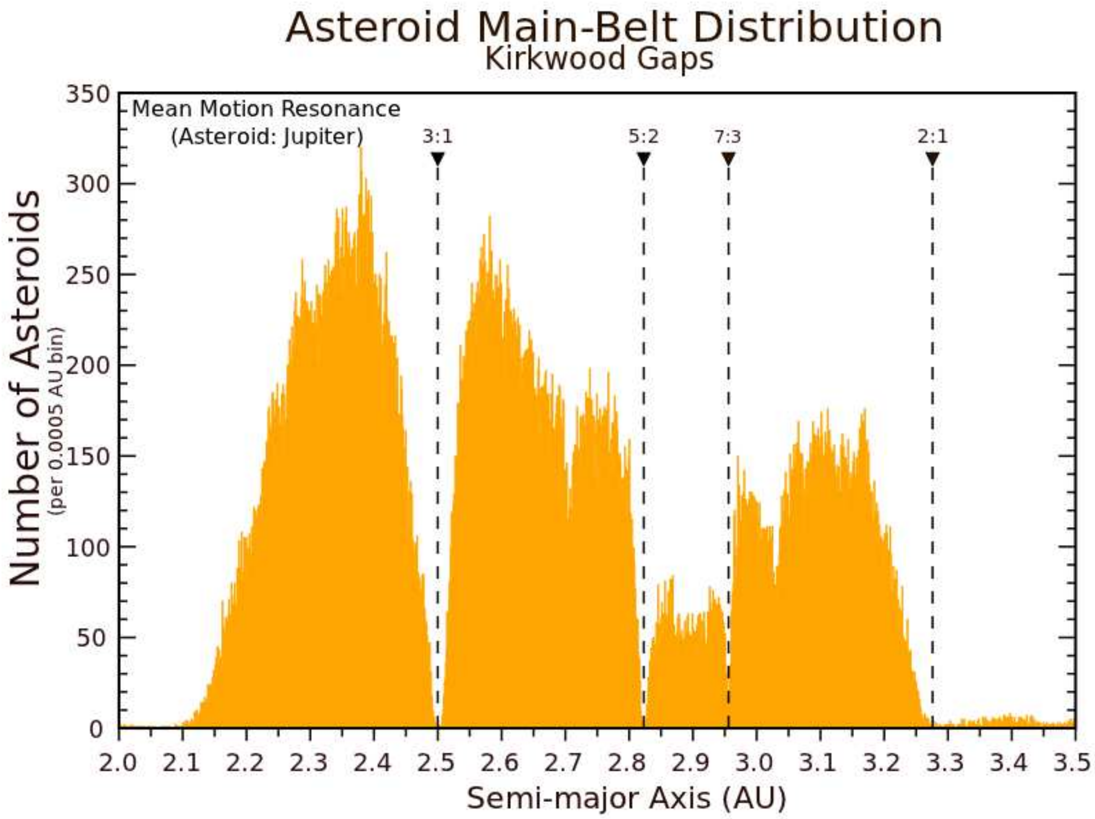

Kirkwood Gaps

- It is believed that these gaps are due to instability mechanisms.
- This motivates us to study the 3:1 resonance

$$a^{3/2} \approx \frac{\omega_J}{\omega_A} = \frac{1}{3}.$$

Theorem 1 (FGKR, 2011) *Consider the* elliptic *RTBP with mass ratio* $\mu = 10^{-3}$ *and eccentricity of Jupiter* $e_0 > 0$.

For e_0 *small enough, there exist* $T > 0$ *and a trajectory whose eccentricity* $e(t)$ *satisfies*

$$e(0) < 0.55 \qquad and \qquad e(T) > 0.85,$$

while its semi-major axis stays almost constant

$$a(t) \approx 3^{-2/3}.$$

Summary of Proof

1. Prove the existence of a normally hyperbolic invariant cylinder Λ, which exists near the resonance.

2. Establish transversality of its stable and unstable invariant manifolds.

3. Compare inner and outer dynamics on Λ, and check that they do not have invariant circles.

4. Construct diffusing orbits by shadowing a composition of outer and inner maps.

- When $\mu > 0$, all known analytical techniques fail to estimate the splitting of separatrices (even for $e_0 = 0$).
- We set $\mu = 10^{-3}$, and we show numerically that the splitting is not too small.
- Since the splitting varies smoothly with respect to e_0, it suffices to estimate the splitting for $e_0 = 0$ (i.e. for the *circular* problem)!!

Ansatz 1 *Consider the* circular *RTBP with mass ratio* $\mu = 10^{-3}$ *and Hamiltonian* H.

In each energy level $H \in [H_-, H_+]$ *there exists a hyperbolic periodic orbit* $\lambda_H(t)$ *which satisfies*

$$|L_H(t) - 3^{-1/3}| < 50\mu \qquad \textit{for all} \quad t \in \mathbb{R}.$$

Each λ_H *has two branches of stable and unstable invariant manifolds* $W^{s,j}(\lambda_H)$ *and* $W^{u,j}(\lambda_H)$ *for* $j = 1, 2$. *For each* $H \in [H_-, H_+]$ *either*

$$W^{s,1}(\lambda_H) \cap W^{u,1}(\lambda_H) \textit{ transversally}$$

or

$$W^{s,2}(\lambda_H) \cap W^{u,2}(\lambda_H) \textit{ transversally.}$$

Comments

- We verify the Ansatz numerically.
- Numerical analysis has several sources of error:
  - roundoff errors in computer arithmetic,
  - numerical approximation of ideal objects.

  We evaluate such errors and check that they are appropriately small.
- Goal: to keep our numerics simple and convincing.
- Roldán and Zgliczynski are working towards a fully rigorous Computer-Assisted proof.

Choice of Coordinates

- Circular RTBP in rotating Cartesian coordinates

$$H(x, y, p_x, p_y) = \frac{1}{2}(p_x^2 + p_y^2) + yp_x - xp_y - \frac{\mu_1}{r_1} - \frac{\mu_2}{r_2},$$

$$r_1^2 = (x - \mu_2)^2 + y^2,$$
$$r_2^2 = (x + \mu_1)^2 + y^2.$$

- Sun is located to the left of the orgin: $\mu_1 = \mu$ is the small mass and $\mu_2 = 1 - \mu$ is the large mass.

Symmetries of the System

- The system is reversible with respect to the involution

$$R(x, y, p_x, p_y) = (x, -y, -p_x, y).$$

- Thus, a solution is symmetric if and only if it intersects the *symmetry plane*

$$\{y = 0,\ p_x = 0\} \quad \equiv \quad \{y = 0,\ \dot{x} = 0\}.$$

Conservation of Energy

- The circular problem has a conserved quantity, the Jacobi constant C.
- When the Hamiltonian is constant $H = H_0$, we have

$$H_0 = -\frac{C - \mu_1\mu_2}{2}.$$

- We will refer to H_0 as the *energy* of the system.
- It is natural to fix $H = H_0$ and perform our analysis for H_0. Then, we let H vary and repeat our computations for $H \in [H_-, H_+]$.

Computation of Periodic Orbits

- Fix $H = H_0$, and look for an (almost) resonant periodic orbit $\lambda_H(t)$ in this level of energy.
- As a first approximation, consider the 2BP and look for the resonant periodic orbit $\tilde{\lambda}_H(t)$ in the level of energy $H_{\mathrm{2BP}} = H_0$.
- To simplify numerics, we choose a *symmetric* periodic orbit.
- Refine $\tilde{\lambda}_H(t)$ into $\lambda_H(t)$ in the R3BP using a Newton method.

Poincaré Map

- Consider the RTBP in Cartesian coordinates.
- Define the *Poincaré section*

$$\Sigma_+ = \{y = 0,\ \dot{y} > 0\}$$

with *Poincaré map*

$$P:\ \Sigma_+ \to \Sigma_+.$$

- On the section, the variable p_y can be elliminated. We can recover it from the energy condition

$$H(x, y, p_x; p_y) = H_0,$$

since $\partial_{p_y} H = \dot{y} \neq 0$.

- Hence, at each energy level, $P = P(x, p_x)$ is a 2-dimensional symplectic map.

Fixed Point Equation

- In the rotating frame, a 3:1 resonant periodic orbit makes 2 turns around the origin.
- One can look for a periodic point $a = (x, p_x)$ of the Poincaré map

$$a = P^2(a),$$

or equivalently, a fixed point of the *iterated Poincaré map* $\mathcal{P}$

$$a = \mathcal{P}(a).$$

- However, we want a *symmetric* periodic orbit. Thus, after half a period, it must intersect the symmetry plane $\{y = 0, p_x = 0\}$:

$$\Pi_{p_x} \circ P(a) = 0.$$

- Solve this 1-d equation using a Newton method.

Family of Periodic Orbits

- Finally, let H vary in the range $[H_-, H_+] = [-1.733, -1.405]$ to obtain the family of (almost) resonant periodic orbits

$$\Lambda_0 = \bigcup_{H \in [H_-, H_+]} \lambda_H .$$

- Λ_0 is a family of symmetric periodic orbits around the Sun.
- Accuracy in the computation of periodic orbits: 10^{-14}.

Family of Periodic Orbits

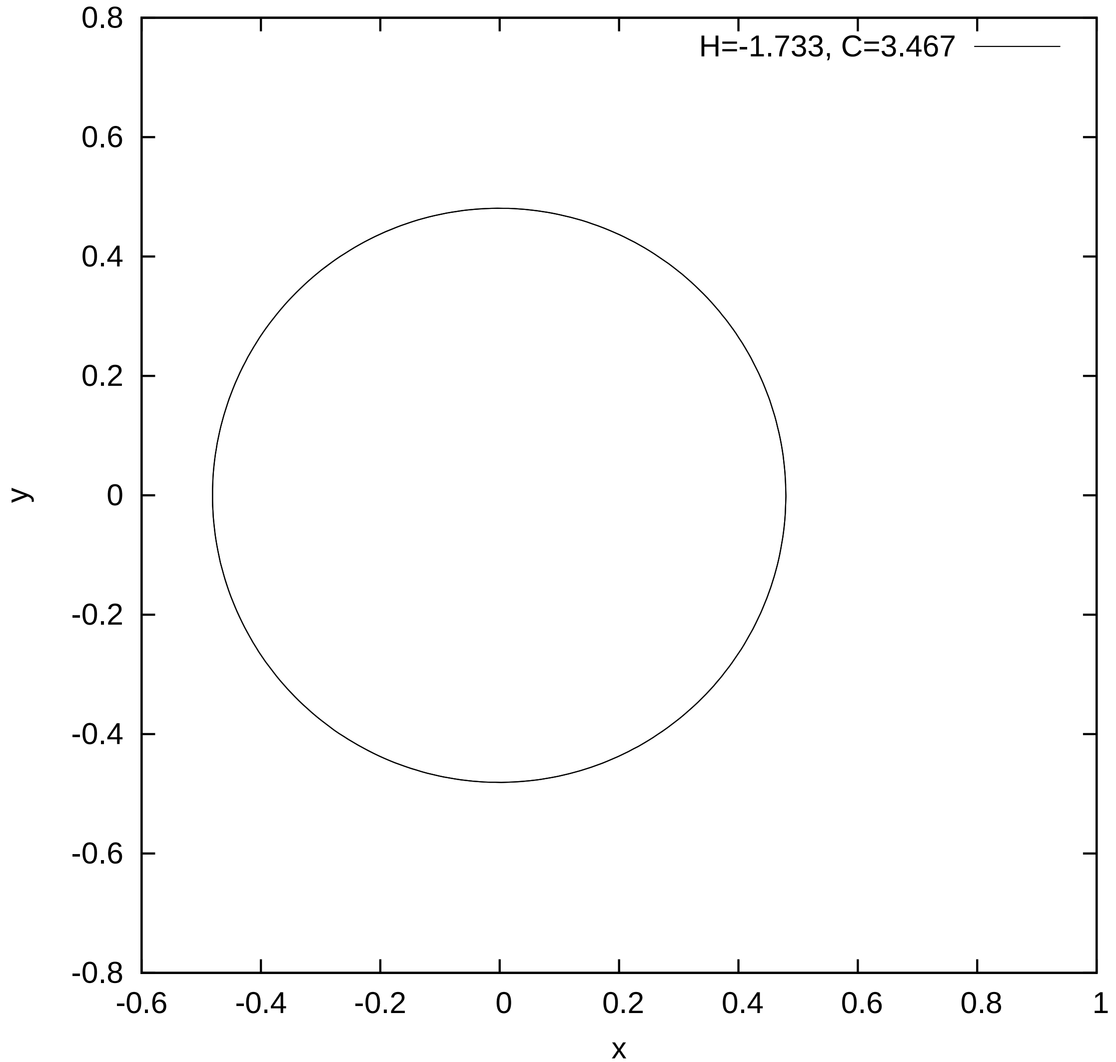

Family of Periodic Orbits

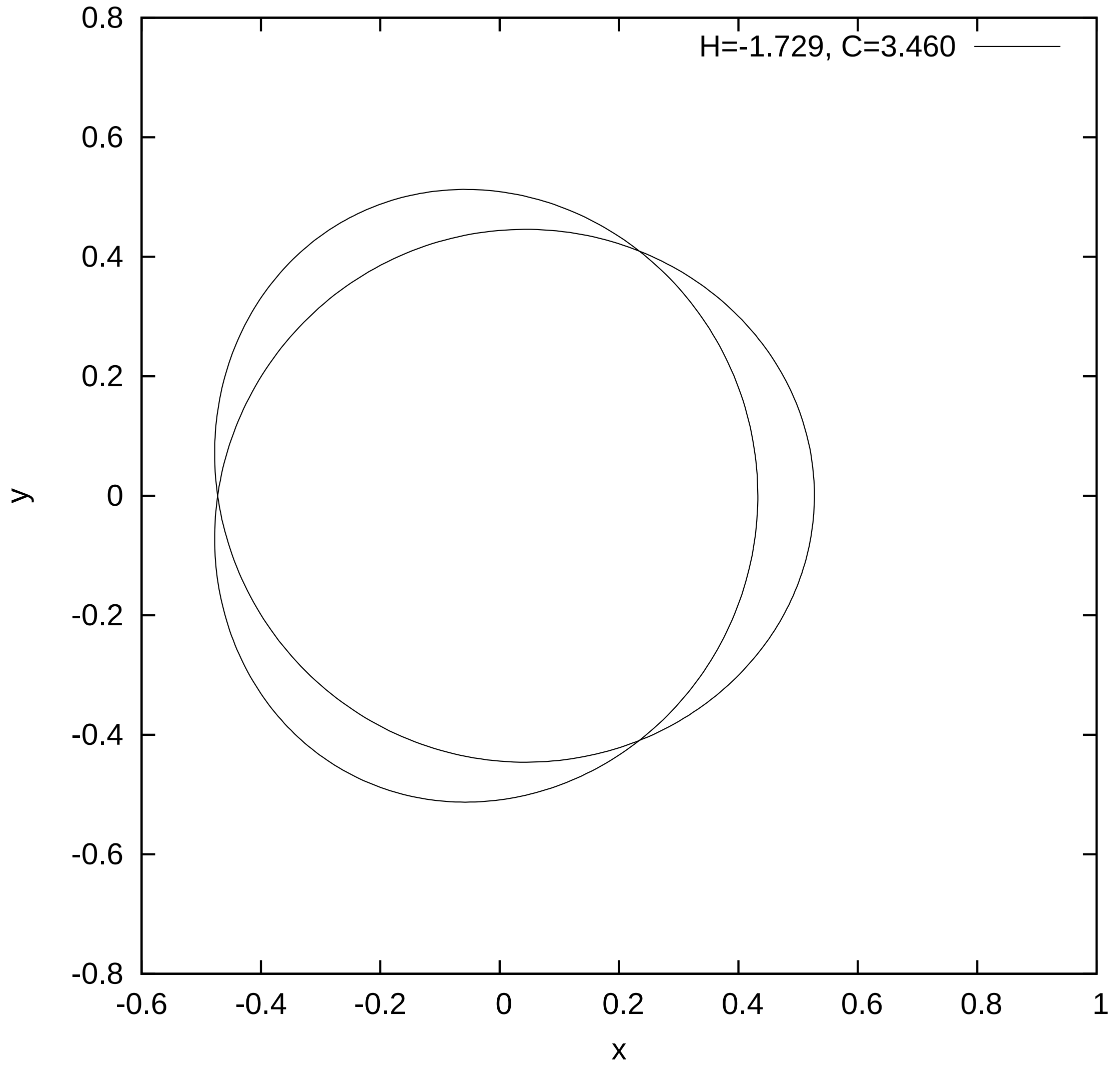

Family of Periodic Orbits

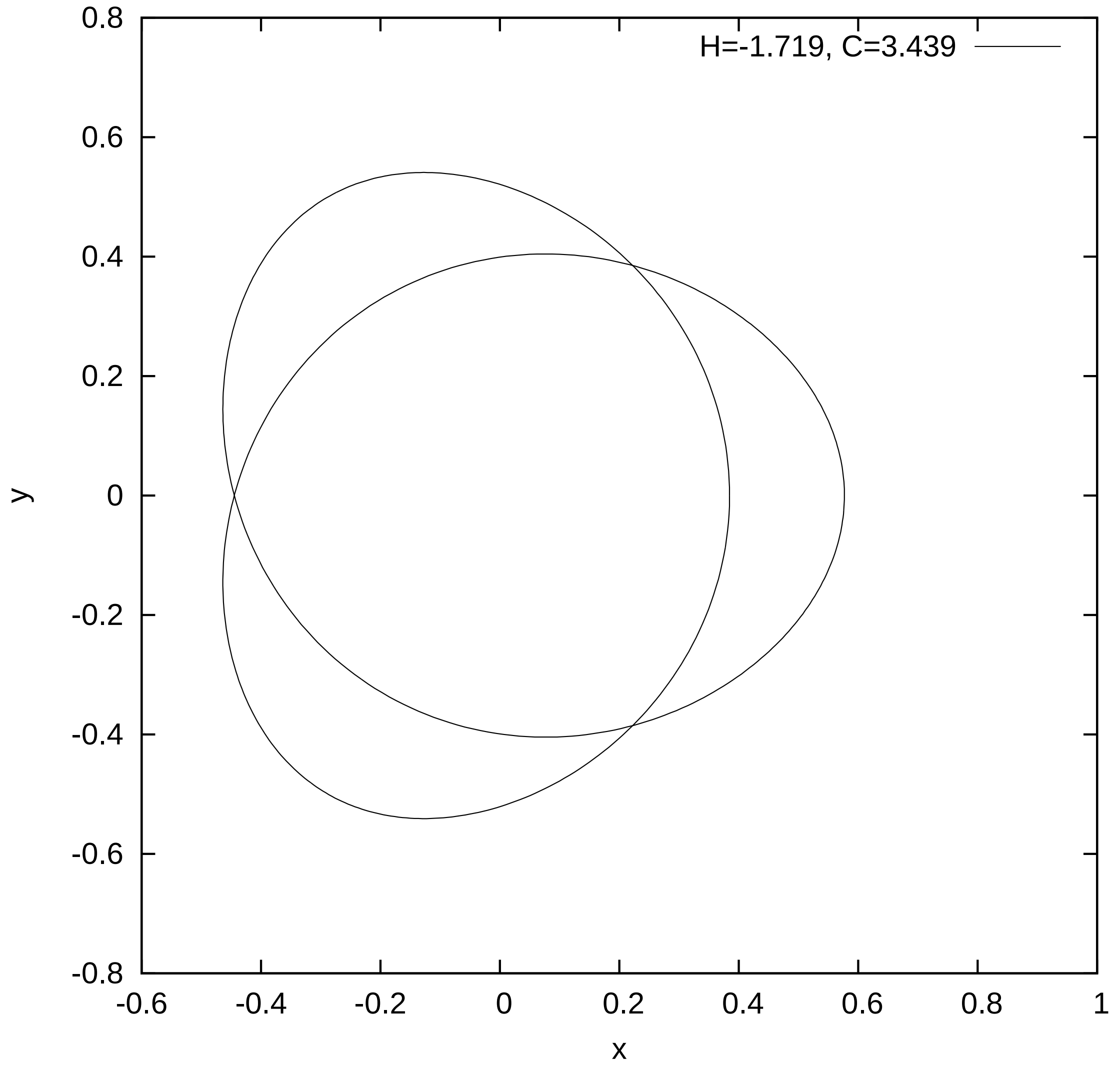

Family of Periodic Orbits

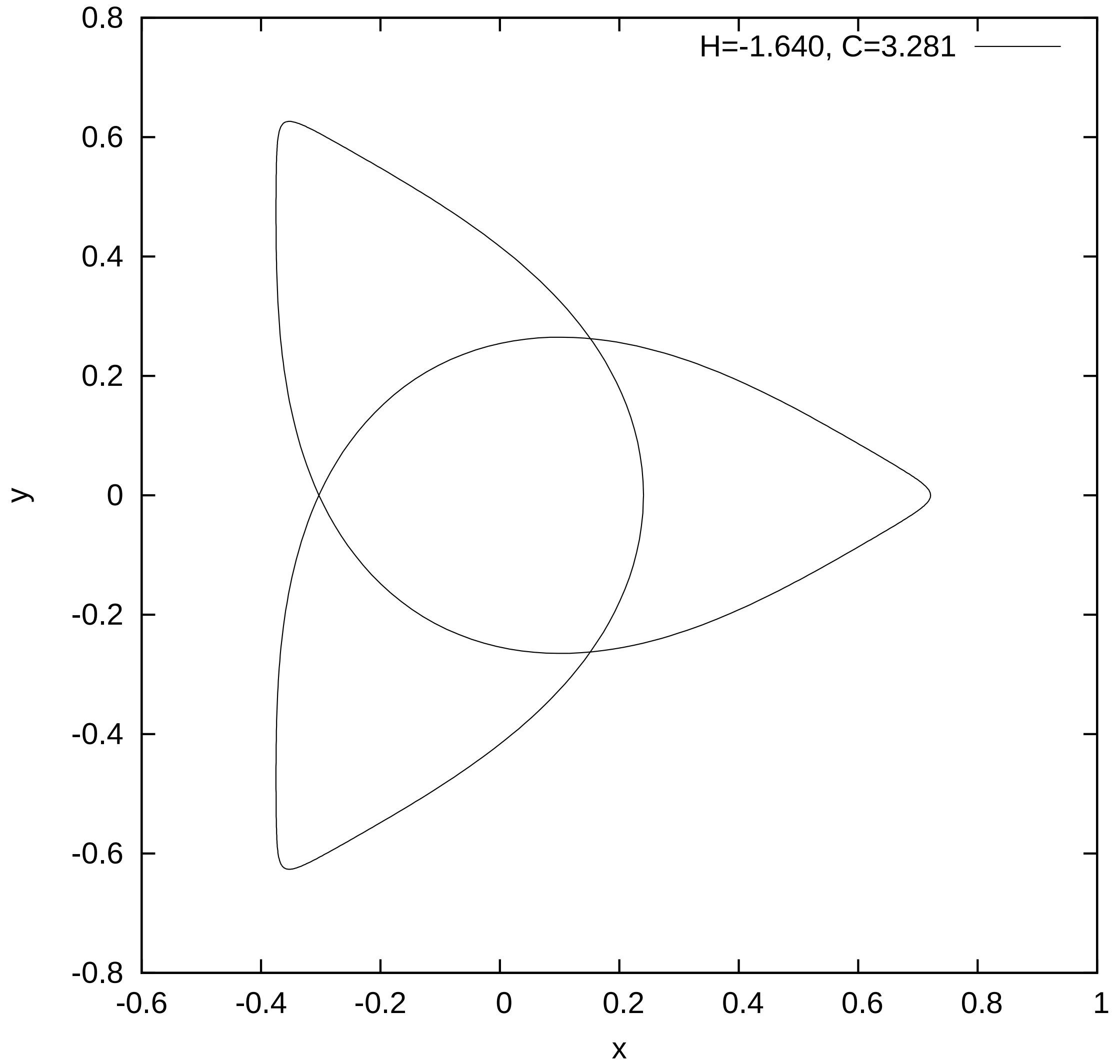

Family of Periodic Orbits

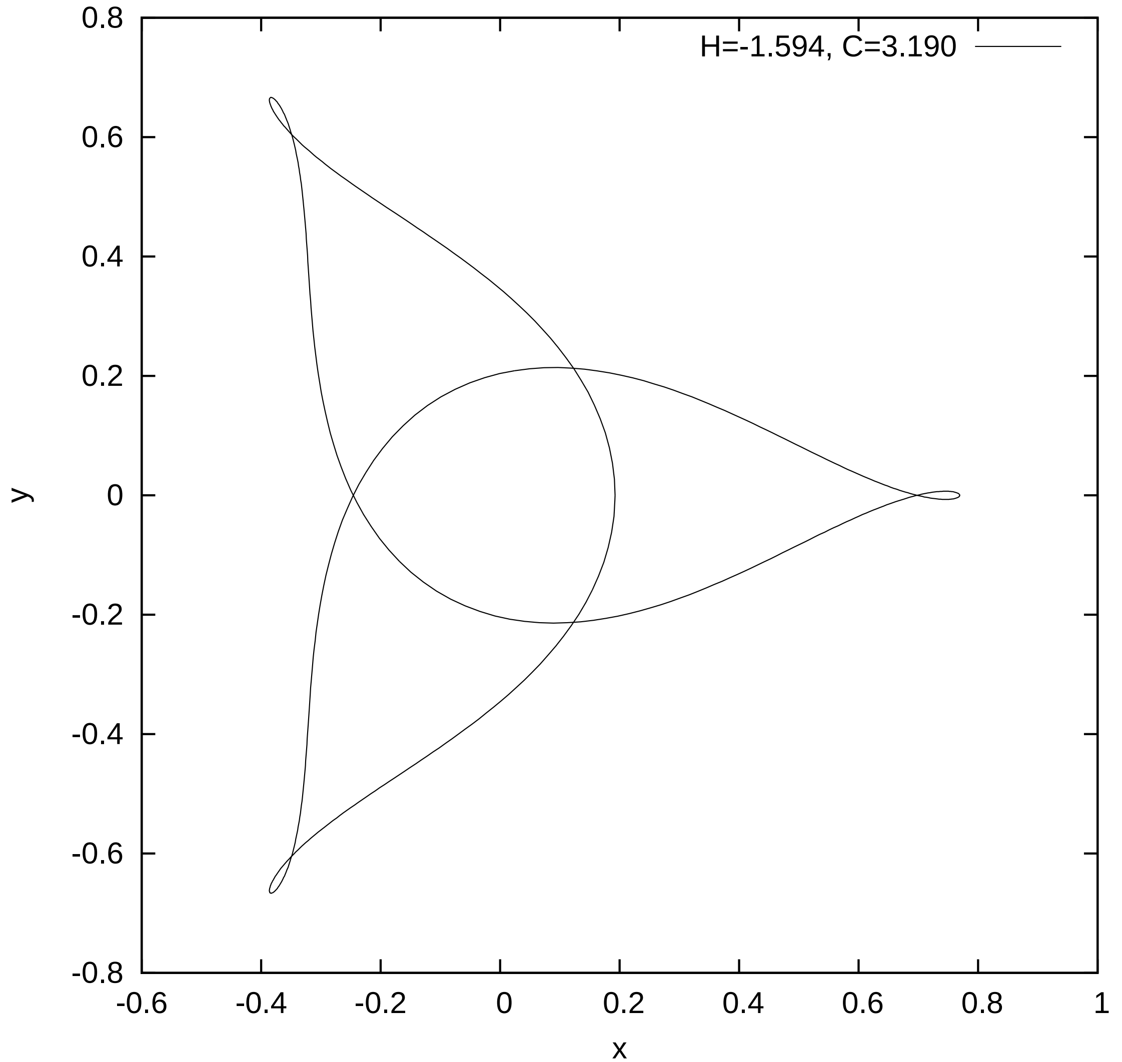

Family of Periodic Orbits

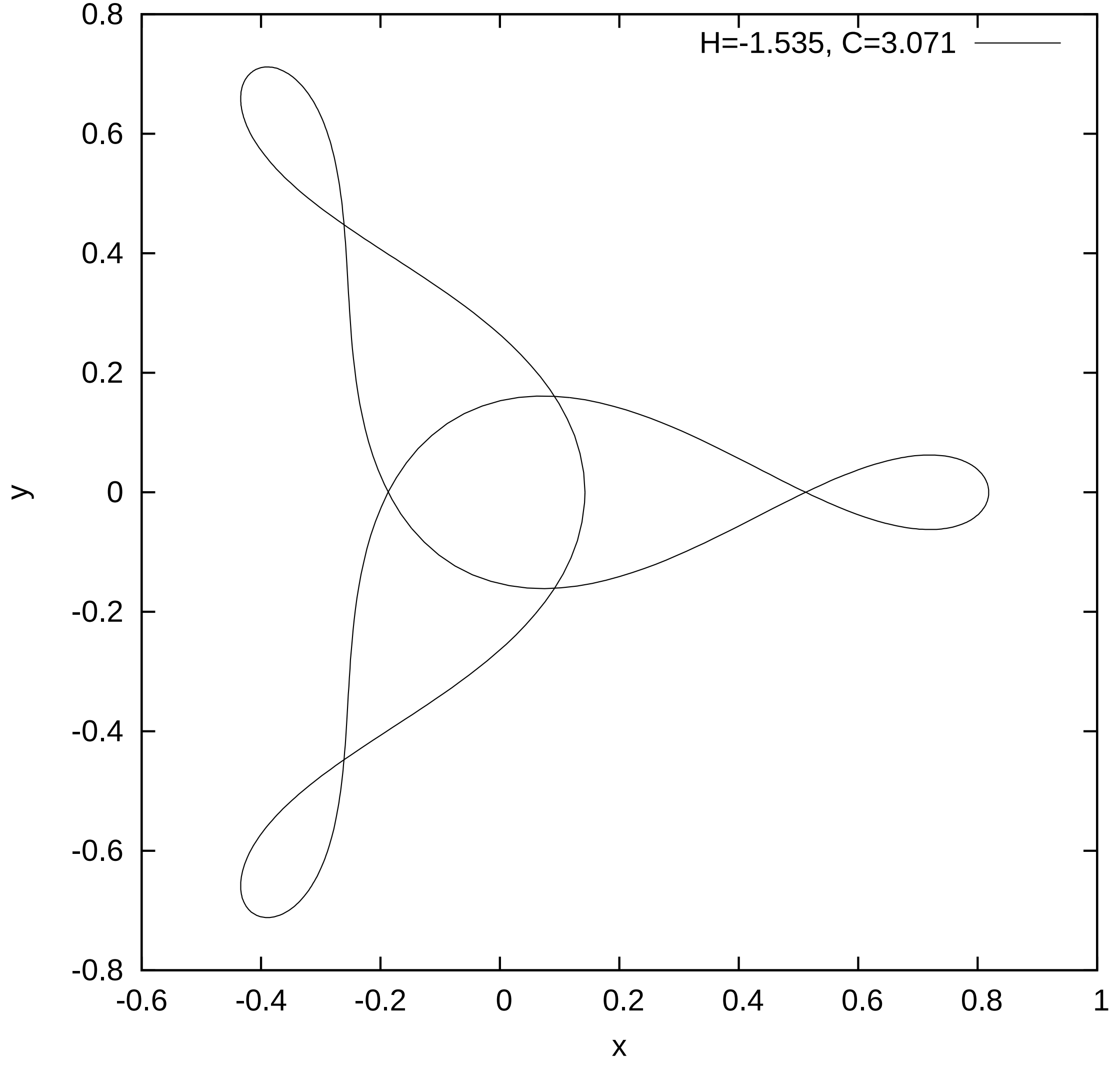

Family of Periodic Orbits

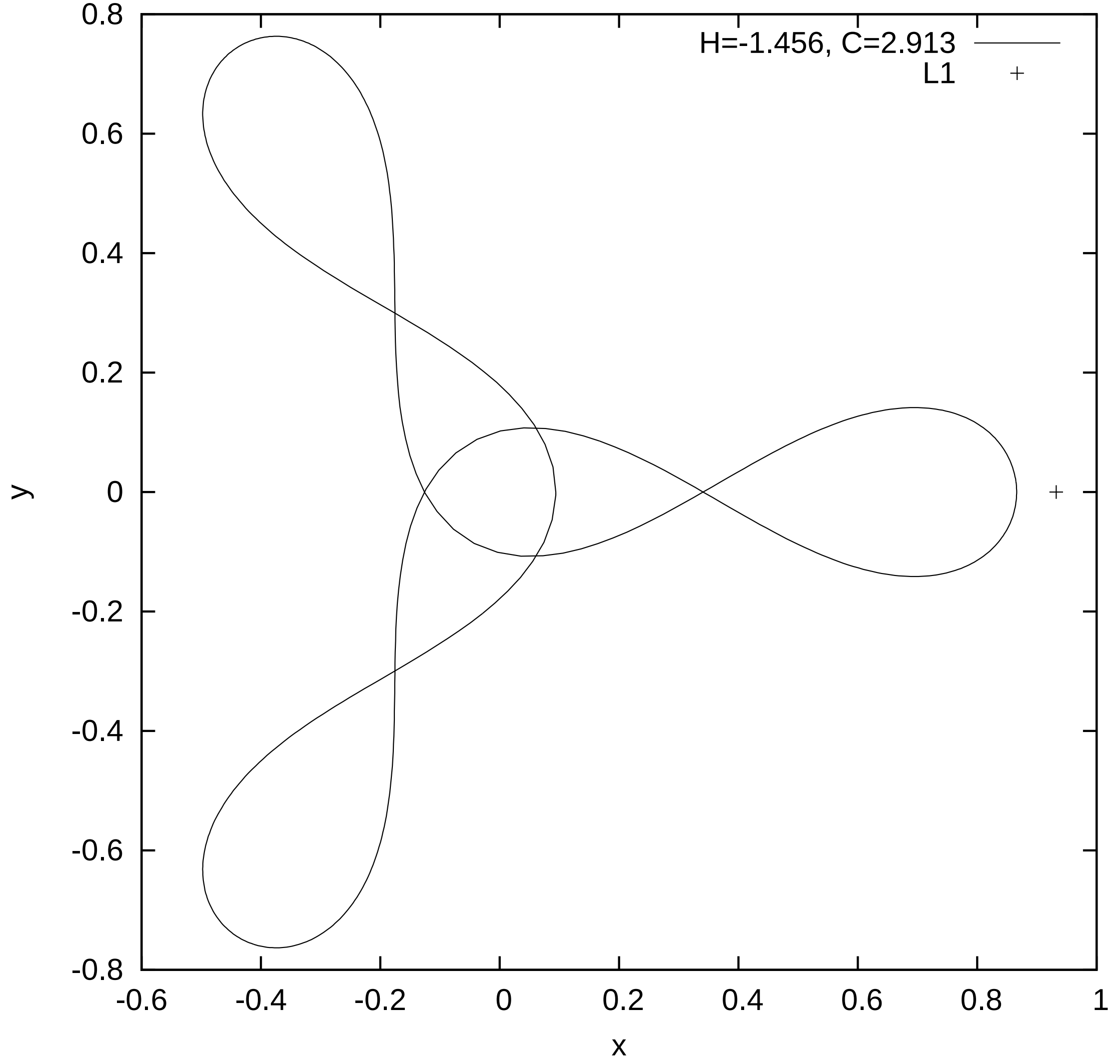

Family of Periodic Orbits

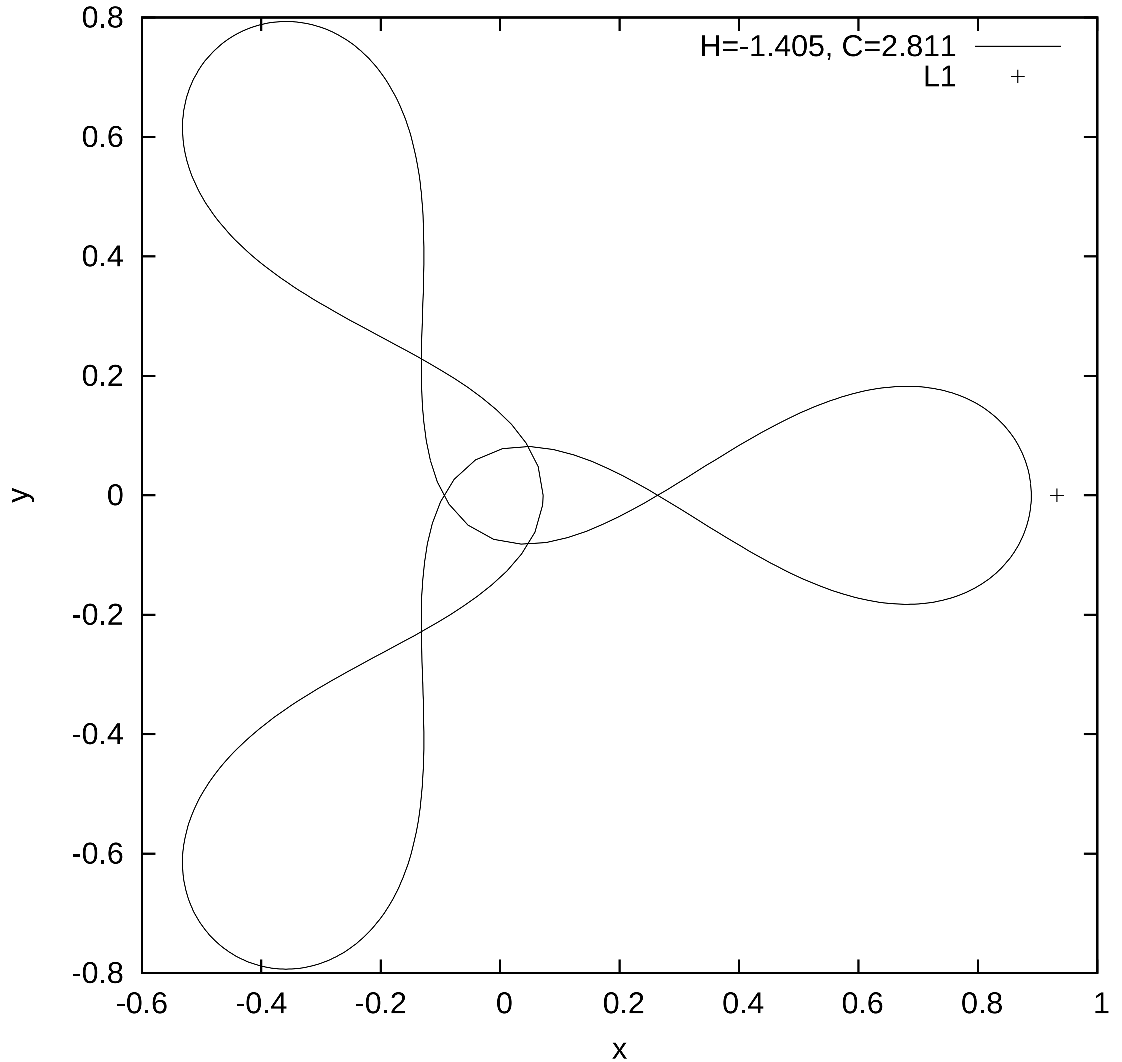

In the Loop

- When $H \approx -1.6$, the periodic orbit develops loops. The reason is the following:
- Near the apohelion, the sideral velocity of Asteroid becomes smaller than the velocity of rotating frame $\Longrightarrow$ relative velocity is negative, and orbit is direct.
- At other parts of the orbit, the sideral velocity of Asteroid is larger than the velocity of rotating frame $\Longrightarrow$ relative velocity is positive, and orbit is retrograde.
- Loops are inherent to this resonant family of periodic orbits in the rotating system, even for the 2BP.

In the Loop

- When the loops appear, there is one more iterate of the Poincaré map. However, the family is continuous with respect to the period T_H.
- This is an artifact produced by rotating coordinates. One can get rid of this technical problem by redefining the Poincaré map in a suitable way.

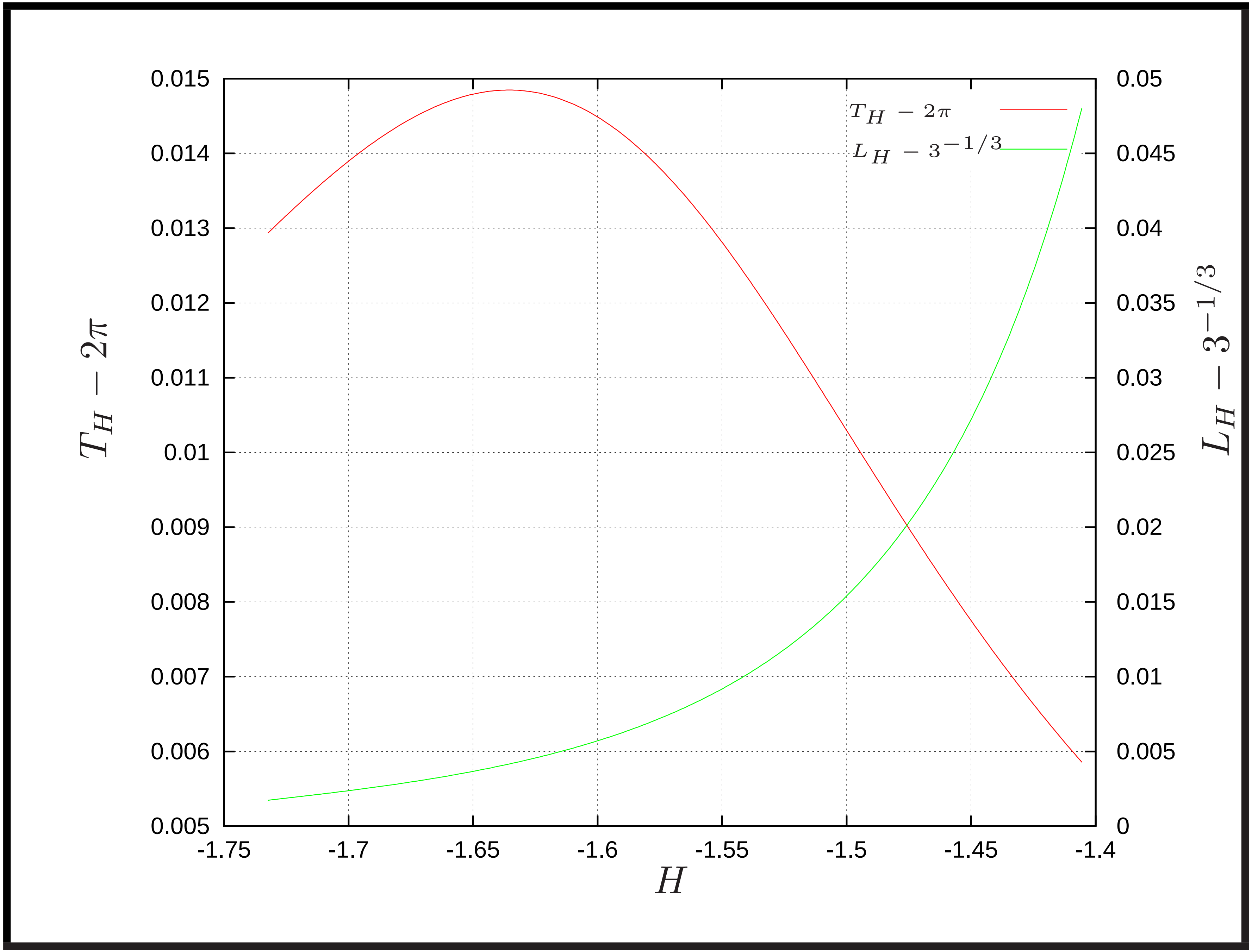

$T_H - 2\pi$
$L_H - 3^{-1/3}$
0.015
0.014
0.013
0.012
0.011
0.01
0.009
0.008
0.007
0.006
0.005
0.05
0.045
0.04
0.035
0.03
0.025
0.02
0.015
0.01
0.005
0
-1.75
-1.7
-1.65
-1.6
-1.55
-1.5
-1.45
-1.4
H

Numerical Bounds

- The period stays close to the resonant period of the unperturbed system

$$|T_H - 2\pi| < 15\mu.$$

- $L_H(t)$ stays close to the resonant value $3^{-1/3}$:

$$\max_{t\in[0,T_H]} |L_H(t) - 3^{-1/3}| < 50\mu.$$

Stability of Periodic Orbits

- Compute eigenvalues λ, λ^{-1} of $D\mathcal{P}(a)$.

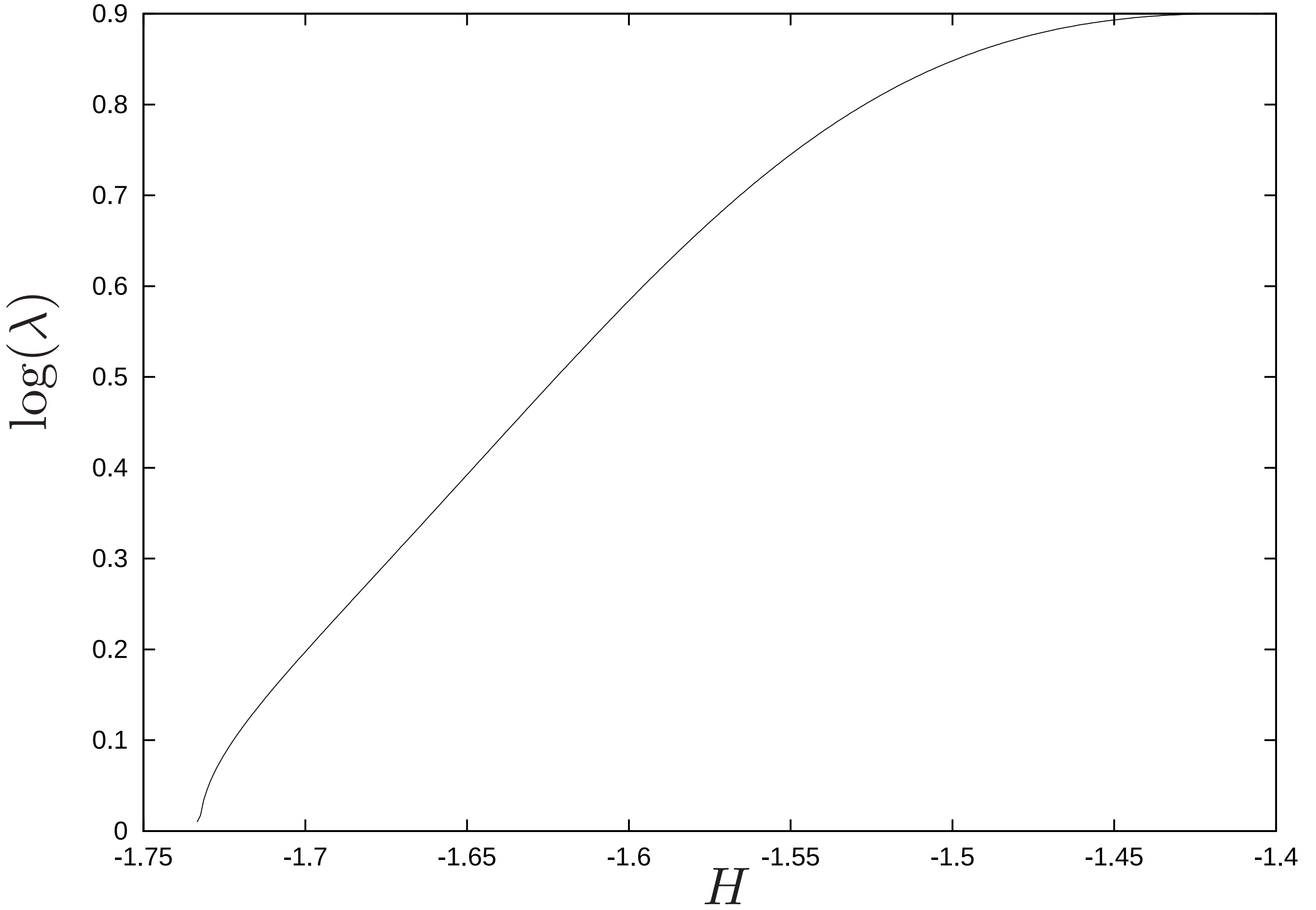

Stability of Periodic Orbits

- The family of periodic orbits is
  - less hyperbolic when $H \to H_-$, or equivalently $e \to 0$.
  - more hyperbolic when $H \to H_+$, or equivalently $e \to 1$.
- Since the system is close to integrable (μ is small), one expects eigenvalues λ, λ^{-1} close to unity.
- Nevertheless, non-integrability is noticeable in the picture. This is due to the effect of the perturbing body (Jupiter) on the Asteroid.

Computation of Invariant Manifolds

- Fix $H = H_0$, and look for the (1-d) invariant manifolds $W^u(a), W^s(a)$ of the hyperbolic fixed point a in this level of energy.
- Approximate the local invariant manifolds using a linear segment. The error commited in the linear approximation is controled:

$$err(\eta) = \|\mathcal{P}(a + \eta v) - (a + \lambda \eta v)\| \in \mathcal{O}(\eta^2).$$

- Globalize the manifolds using the Poincaré map.
- Choose a displacement η such that $err(\eta) < 10^{-8}$ uniformly in H.

Invariant Manifolds for $H = -1.733$

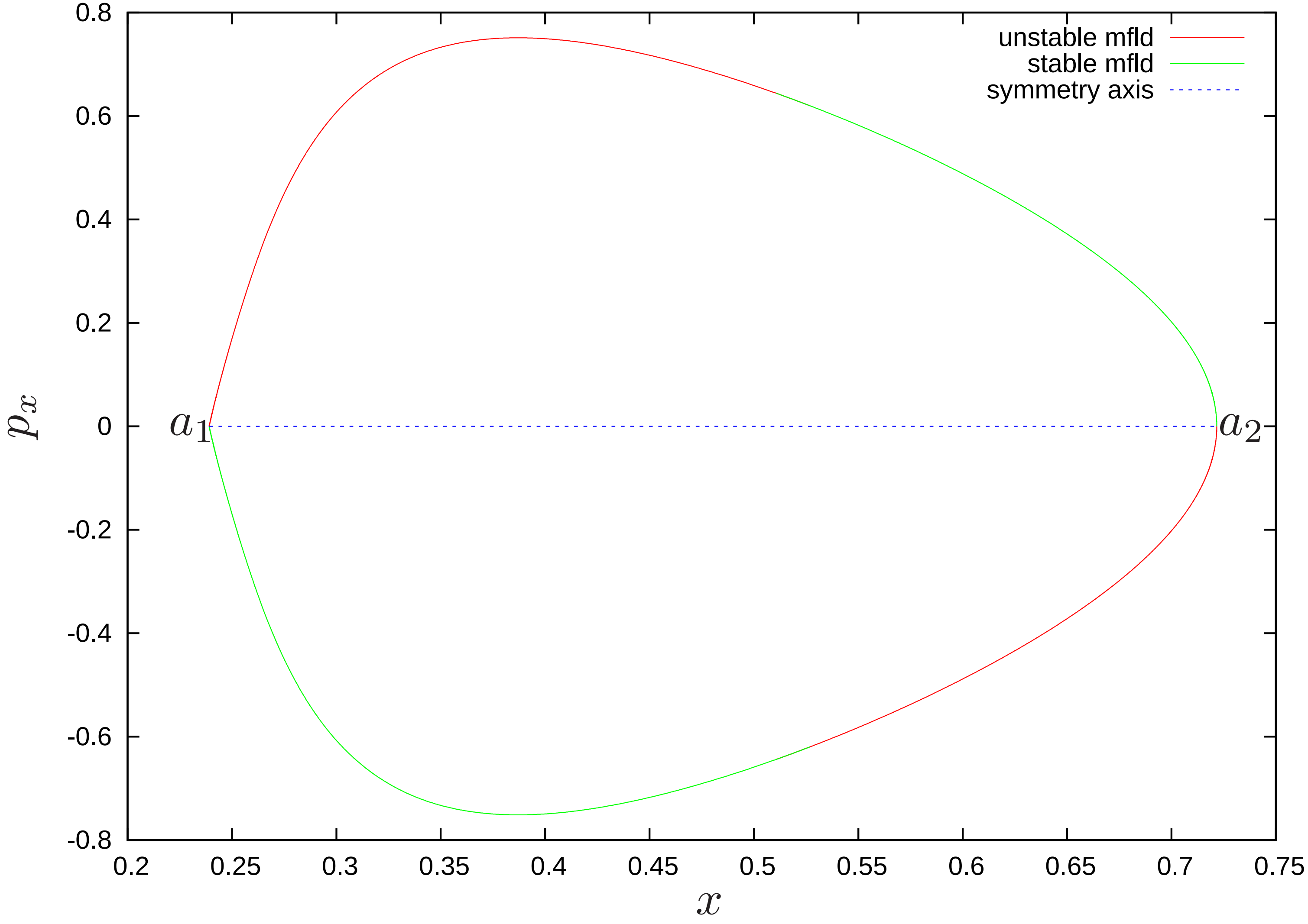

New Poincaré Section

- Notice that the fixed points a_1, a_2 are in the symmetry plane by construction.
- Unfortunately, the homoclinic points are *not* in the symmetry plane.
- Consider the new Poincaré section

$$\Sigma_- = \{y = 0, \dot{y} < 0\}.$$

- In the new section Σ_-, the fixed points a_1, a_2 are reversible:

$$R(a_1) = a_2.$$

  Hence, the homoclinic points are now in the symmetry plane.

Invariant Manifolds on the section Σ_-

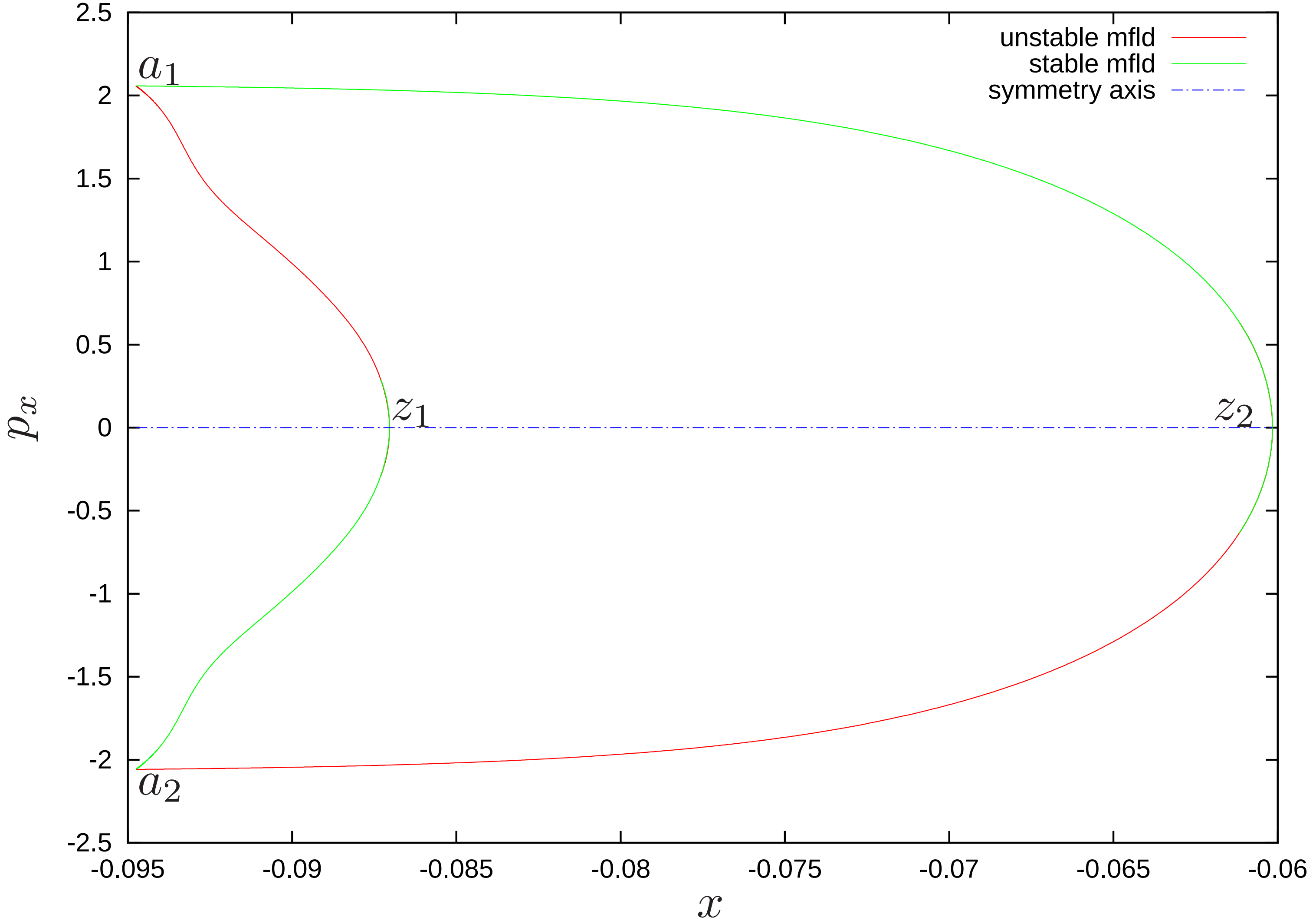

Homoclinic Points

- Thanks to reversibility, the intersection of the manifolds with the symmetry axis $p_x = 0$ is a homoclinic point.
- We consider two homoclinic points:
  - z_1 corresponds to the “inner” splitting,
  - z_2 corresponds to the “outer” splitting.
- Compute z_1, z_2 using a standard bisection method.
- We verify that z_1, z_2 lie on the symmetry axis with tolerance 10^{-10} uniformly in H.

Inner Splitting for $H = -1.405$

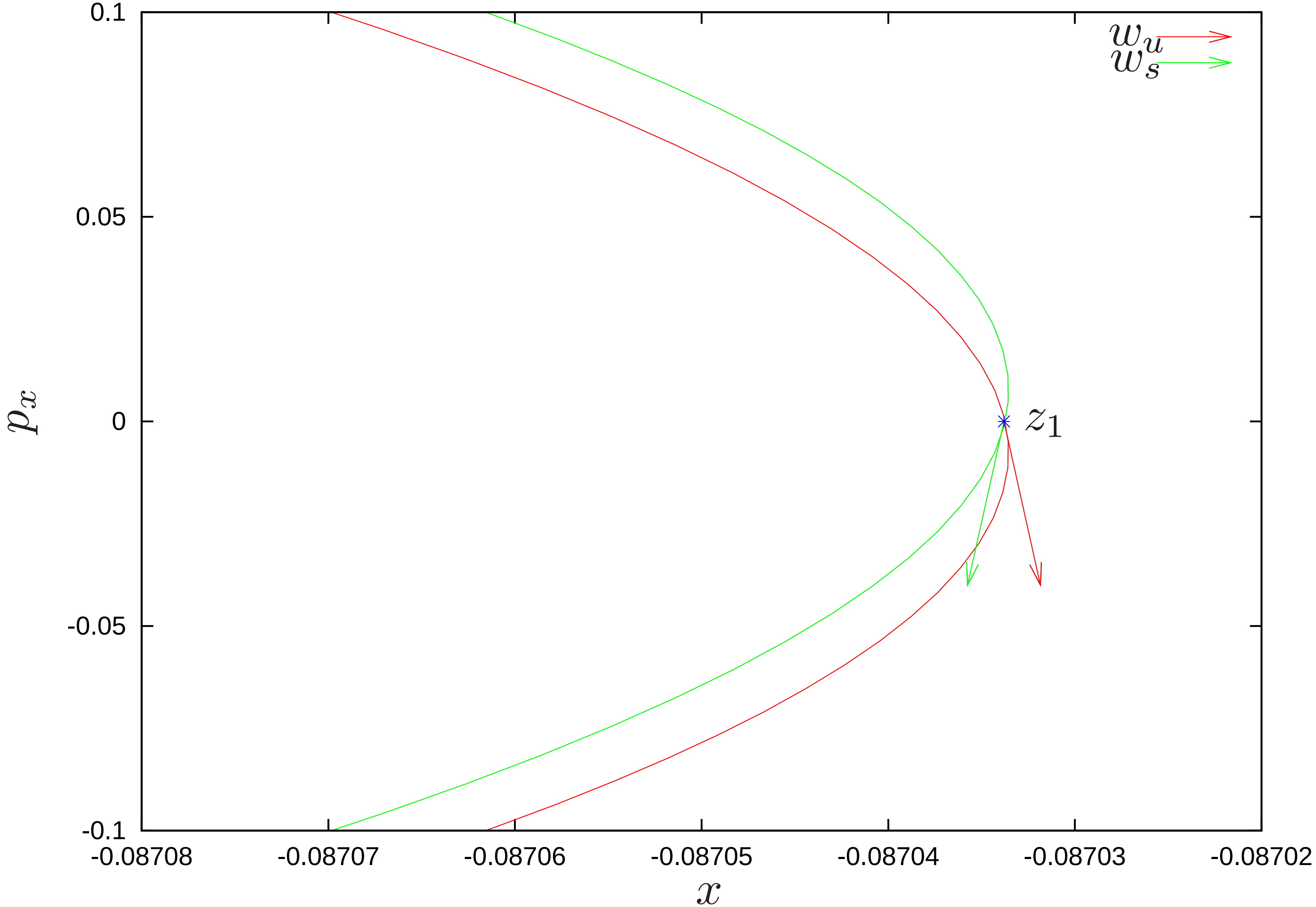

Computation of Splitting Angle

- Look for the tangent vectors w_u and w_s to the manifolds at z. The *splitting angle* is the oriented angle between them.
- We use two different methods to compute the tangent vectors at z. This way we can validate the numerical accuracy of the splitting angle.

First Method

- Let $p_0 \in W^u_{\text{loc}}(a)$ be the preimage of the homoclinic point z in the local manifold

$$\mathcal{P}^n(p_0) = z.$$

- Let v_0 be the tangent vector to the manifold at p_0 (i.e. the eigenvector).

- Transport v_0 by the Jacobian $D\mathcal{P}$ at the successive iterates of p_0

$$w_u = \prod_{i=0}^{n-1} D\mathcal{P}(p_i) v_0.$$

Second Method

- Let $z = (x^*, 0)$ be the homoclinic point.
- Look at the manifold $W^u(a)$ as a graph over the vertical line $x = x^*$.
- Sample the manifold $W^u(a)$ at different values of p_x:

$$p_x = \frac{j}{10^5}, \qquad j \in (-2, -1, 1, 2).$$

- Apply numerical differentiation to these values, using central differences centered at $p_x = 0$:

$$d_1 = \frac{x(0.00001) - x(-0.00001)}{0.00002},$$

$$d_2 = \frac{x(0.00002) - x(-0.00002)}{0.00004}.$$

- Use Richardson extrapolation to improve the precision of derivative:

$$d = \frac{4d_1 - d_2}{3}.$$

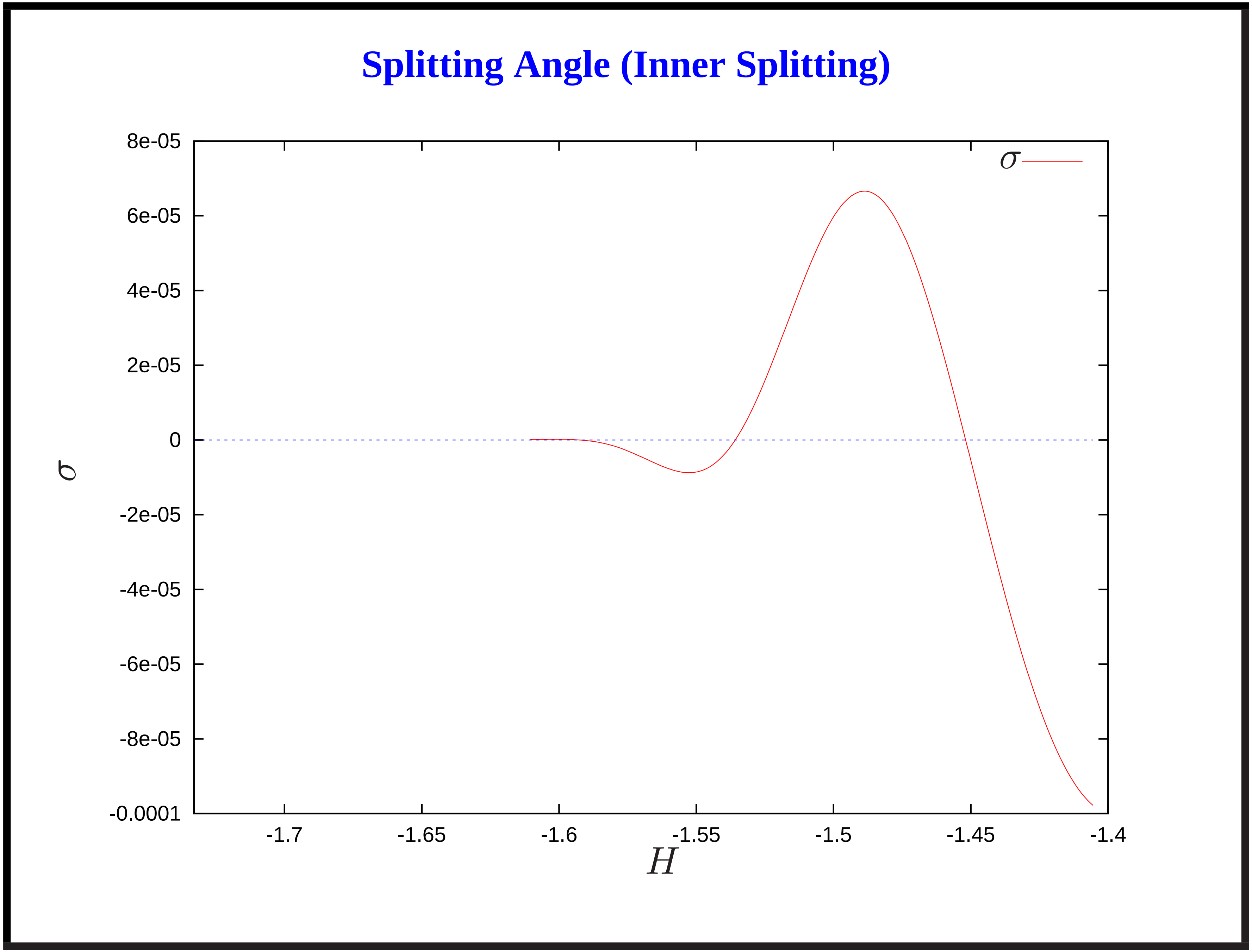
Splitting Angle (Inner Splitting)
8e-05
6e-05
4e-05
2e-05
0
-2e-05
-4e-05
-6e-05
-8e-05
-0.0001
-1.7
-1.65
-1.6
-1.55
-1.5
-1.45
-1.4
H
σ
σ

Accuracy of Computations

- Let $H = H_0 = -1.405$, for example.
- According to the first method, the splitting angle is $\sigma^{(1)} = -9.780327341442923e - 05$.
- According to the second method,

p_x	x^u
-0.00002	$-8.703373796876306e - 02$
-0.00001	$-8.703373845681261e - 02$
0.00001	$-8.703373943484494e - 02$
0.00002	$-8.703373992482412e - 02$

$$
\begin{aligned}
d_1 &= -4.890161608983589e-05 \\
d_2 &= -4.890152657810453e-05 \\
d &= -4.890164592707968e-05 \\
\sigma^{(2)} &= -9.780329177619804e-05
\end{aligned}
\tag{1}
$$

- Compare the splitting angle computed using the two methods:

$$
\begin{aligned}
\sigma^{(1)} &= -9.780327341442923e-05, \\
\sigma^{(2)} &= -9.780329177619804e-05.
\end{aligned}
\tag{2}
$$

They differ by less than 10^{-10} (total numerical error).

Validation of Splitting Angle

- The splitting angle is several orders of magnitude larger than the total numerical error for a large range of energies $H \approx [-1.6, -1.4]$.